

# Effect of finely-layered stiff carbonates on a seismic response. Northern Carnarvon basin synthetic study

Anastasia Pirogova\*

Curtin University  
26 Dick Perry Ave,  
Kensington WA 6151  
a.pirogova@postgrad.curtin.edu.au

Roman Pevzner

Curtin University  
26 Dick Perry Ave,  
Kensington WA 6151  
R.Pevzner@curtin.edu.au

Boris Gurevich

Curtin University, CSIRO  
26 Dick Perry Ave,  
Kensington WA 6151  
B.Gurevich@curtin.edu.au

Sergey Vlasov

Santos  
60 Flinders Street  
Adelaide SA 5000  
Sergey.Vlasov@santos.com

## SUMMARY

Fine layering is known to cause both seismic attenuation and VTI-anisotropy. In typical geological environments, the contrast in elastic properties of adjacent layers rarely exceeds 30% so that the layer-induced effects are negligible. However, it's not true for the overburden of Northern Carnarvon basin (Northwest shelf of Western Australia) that is characterized by very stiff carbonates alternated with more porous and softer rocks.

In this paper, we present a workflow for preliminary analysis of seismic wavefield and, in particular, effects of layer-induced scattering attenuation and anisotropy in the target area. The workflow is based on the walk-away VSP full-wave modelling (5-100 Hz) for the flat-layered elastic models that are constructed using logs of four wells, namely, Dampier 1, Parker 1, Wilcox 2 and Withnell 1.

We show that particular sequences with carbonates produce significant amplitude loss and degradation of spectrum of a transient seismic pulse. Maximum attenuation is observed for Withnell 1 borehole and is characterized by the drop of 30% in the centroid frequency in the 200 m interval. Anellipticity parameter  $\eta$  is estimated by fitting of the moveout curves and varies from 0.1 to 1.5. In addition, the modelling reveals a very complex wavetrain with energetic reflected and converted waves at large offsets. All these effects should be taken into account in seismic processing and imaging.

**Key words:** layer-induced, seismic attenuation, VTI anisotropy, carbonates, Northern Carnarvon

## INTRODUCTION

The Northern Carnarvon basin is a premier offshore hydrocarbon province of Australia that has been actively explored and exploited over the recent years. Major prospects in the area are associated with Mesozoic sandstone reservoirs in Triassic Mungaroo, Jurassic Brigadier formations, Lower Cretaceous Barrow group (typical depths are > 2.5 km). The whole basin is overlayed by a thick predominantly carbonate wedge, in which particular intervals are characterized by a high contrast of elastic properties between adjacent fine layers of stiff carbonates and softer rocks.

Fine-layering in high-contrast geological environments is known to cause scattering of propagating seismic waves ([O'Doherty and Anstey, 1971](#)) and VTI-anisotropy ([Backus, 1962](#)). Since both phenomena affect a seismic image, they should be properly modelled, analysed and taken into account at the stage of a survey design.

In this paper, we quantitatively evaluate layer-induced effects from the carbonate formations in the Dampier sub-basin and the Ranking platform using logs of four wells, namely, Dampier 1, Parker 1, Wilcox 2 and Withnell 1. The study is based on synthetic full-wave elastic modelling for a walk-away VSP survey geometry. Scattering attenuation is defined in terms of quality-factors Q computed by a modified centroid frequency shift method (CFS). P-wave anisotropy is evaluated through the anellipticity parameter  $\eta$  by least-square fitting of travel-time curves.

## FULL-WAVE ELASTIC 1D MODELLING

In order to analyse effects of fine-layering, very high-resolution models available from density and sonic logs (resolution of 0.15 m) were utilized for the full-wave seismic simulation. For Withnell 1, the density profile was built from the sonic logs using the Gardner equation. Prior to the simulation, the logs were upscaled up to 1 m using Backus effective medium theory. Figure 1 demonstrates the initial and the upscaled P-wave velocity logs for the overburden (up to 1.8 km) of Dampier 1, Parker 1, Wilcox 2 and Withnell 1 wells.

The logs indicate that each borehole crosses a thick formation characterized by a strong contrast of elastic properties. Within this formation high-impedance fine layers ( $V_p > 5 \text{ km/s}$ ,  $\rho > 2.4 \text{ kg/m}^3$ ) are alternated with beds of drastically lower velocities and densities. For particular intervals the contrast in properties exceeds 100 %.

According to lithology columns the high-impedance formation has predominantly carbonate composition (calcarenite, calcilutite, dolomites).

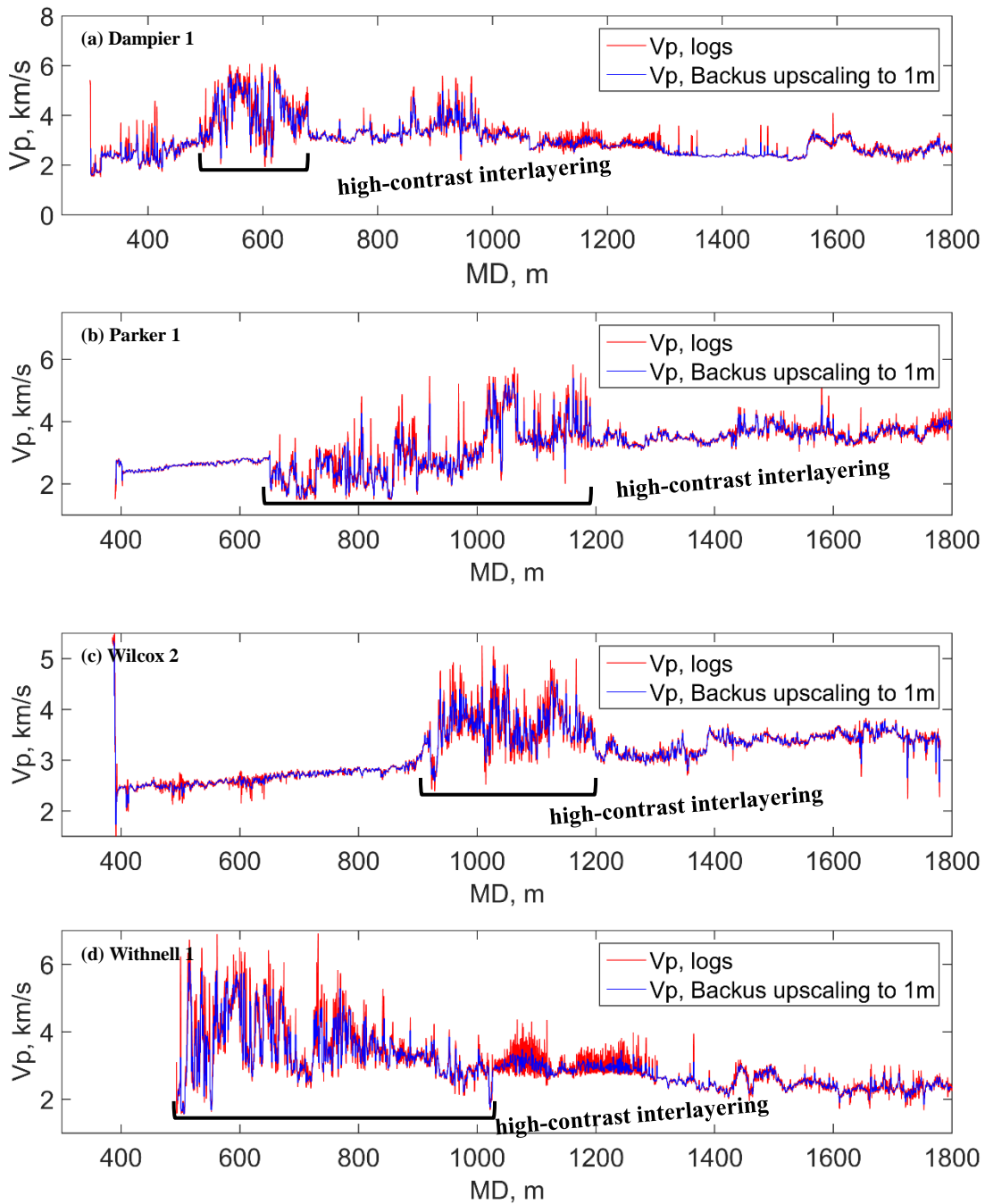


**Figure 1. P-wave velocity profile from sonic logging; (a) Dampier 1, (b) Parker 1, (c) Wilcox 2 and (d) Withnell 1.**

Multicomponent seismic wavefield was generated for the flat-layered elastic models by 2D OASES code based on wavenumber integration in combination with the Direct Global Matrix solution technique ([Schmidt and Tango, 1986](#)). Given a selection of frequencies, the code computes a depth-dependent Green-function (transfer function) by evaluation of a wavenumber integral at any receiver position. In our synthetic study, seismograms were obtained by the convolution of the calculated transfer function with the pulse collected from the field VSP dataset (5-100 Hz frequency range).

For the computational purpose, the logs were extrapolated from the given level to the sea surface. The acoustic properties of the water column were assumed to be constant ( $V_p = 1540 \text{ m/s}$ ,  $\rho = 1000 \text{ kg/m}^3$ ). The geophones were equidistantly distributed with a 5 m interval from the sea surface level. To emulate an airgun excitation, the source was modelled as a compressional explosive type. The array of 149 point sources was suspended 5 m below the sea surface in the direction perpendicular to the depth axis. The minimum and maximum source offsets were 50 m and 3750 m accordingly.

The configuration described above facilitated analysis of 2D walk-away VSP (vertical seismic profiling) and surface seismic gathers. The latter was achieved by the application of a reciprocity principal to the computed VSP seismograms. In this paper we will discuss the synthetic data only for the VSP survey geometry. An example of the computed walk-away VSP gathers is given on Figure 2.

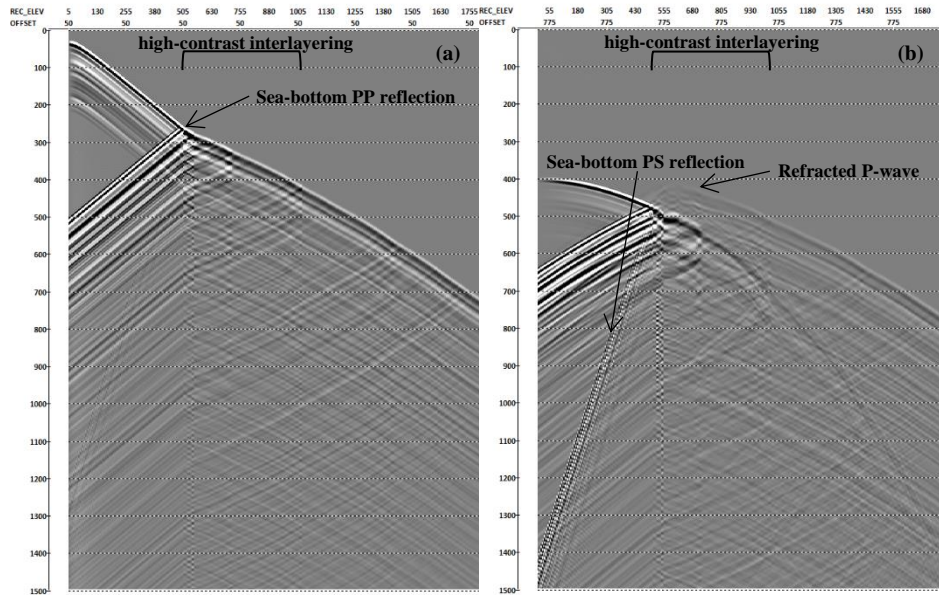


**Figure 2.** Synthetic common-shot-point VSP gathers (vertical component of a particle velocity) computed for Withnell 1 elastic model; (a) source offset 50 m, (b) source offset 775 m. Vertical axis is in ms. Horizontal axis is the depth axis of the borehole (in m).

## LAYER-INDUCED ATTENUATION

VSP has always been the choice method for the analysis of seismic attenuation. In this study, we computed P-wave apparent attenuation from the vertical component of the zero-offset VSP seismogram. We used a concept of a constant quality-factor  $Q$  that characterizes a linear behaviour of an attenuation coefficient over the frequency band. Interval  $Q$ -values along the borehole were computed by the modified centroid frequency shift method (CFS). This method is based on the observation that attenuation causes a linear decrease of a centroid frequency in constant- $Q$  media. Thus a  $Q$ -factor can be defined through the proportionality constant that characterizes this linear decrease ([Quan and Harris, 1997](#)). [Pevzner, et al. \(2012\)](#) modified the original formula for non-Gaussian amplitude spectra:

$$2 \frac{f_{R1} - f_{R2}}{\sigma_{R1}^2 + \sigma_{R2}^2} = \int_{ray} \frac{\pi}{Qv} dl \quad (1)$$

where  $f_{R1}$  and  $f_{R2}$  – centroid frequency,  $\sigma_{R1}^2$  and  $\sigma_{R2}^2$  – variance of amplitude spectra at the first and the second receiver accordingly,  $Q$  – quality-factor estimated between the two receivers,  $v$  – propagation velocity.

Analysis of spectra evolution along the borehole – decay of a centroid frequency in our case – was carried out on the direct arrivals of a P-wave at each receiver level. Prior to the analysis, the spectra were corrected for divergence and the upgoing reflected waves were suppressed by means of FX deconvolution.

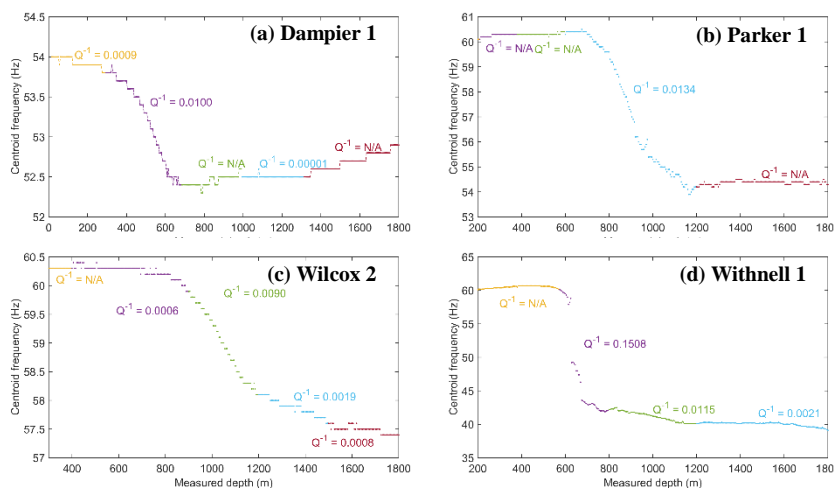


**Figure 3.** Centroid frequency curves and block  $Q^{-1}$ -models (intervals of  $Q^{-1}$  are shown in colour) for (a) Dampier 1, (b) Parker 1, (c) Wilcox 2 and (d) Withnell 1 wells.  $Q^{-1}=N/A$  indicates insensitivity of CFS method (negligible attenuation).

The obtained centroid frequency curves exhibit a prominent decay at the intervals of a high-contrast interlayering. For Dampier 1, Parker 1, Wilcox 2 the decay does not exceed 6 Hz though, while for Withnell 1 scattering on the stack of carbonate layers leads to the frequency drop of a nearly 20 Hz in the 200 m interval. By choosing boundaries, a block-model of  $Q$  values was calculated from the frequency decay curves (see Figure 3). According to this  $Q$ -model, contribution of scattering attenuation for Wilcox 2 and Dampier 1 wells is estimated as  $Q \approx 100$ , for Parker 1  $Q$  is nearly 75, for Withnell 1  $Q \approx 7$  at 600-800 m and  $Q \approx 85$  at 800-1200 m. In addition, other sections of the overburden, which aren't associated with high contrasts of constituent layers, almost do not contribute to the apparent attenuation of propagating waves ( $Q > 450$ ).

## LAYER-INDUCED VTI-ANISOTROPY

As well-known, anisotropy causes a non-hyperbolic behaviour of seismic reflections. Provided the medium is anisotropic NMO velocity analysis based on a hyperbolic moveout equation loses accuracy with an increasing source-receiver offset. The difference between hyperbola and a travel-time curve in anisotropic medium usually becomes pronounced for large offsets that exceed the propagation depth to the reflector ([Tsvankin, 2012](#)).

Horizontally-layered media with prominent contrasts between the layers induce anisotropy with VTI symmetry ([Backus, 1962](#)). Having assumed that the stiff carbonate formation in the overburden of Northern Carnarvon basin has a flat-layered structure, we estimated its anisotropy features. We expressed VTI-anisotropy in terms of anellipticity parameter  $\eta$ :

$$\eta = \frac{\varepsilon - \delta}{1 + 2\delta}, \quad (2)$$

$$\varepsilon = \frac{C_{11} - C_{33}}{2C_{33}}, \quad (3.1)$$

$$\delta = \frac{(C_{13} + C_{44})^2 - (C_{33} + C_{44})^2}{2C_{33}(C_{33} - C_{44})}, \quad (3.2)$$

where  $\varepsilon$  and  $\delta$  are Thomsen parameters (1986),  $C_{ij}$  – components of elastic modulus matrix.

To evaluate anellipticity  $\eta$ , we applied two different approaches: 1) straightforward calculation of Thomsen parameters and the anellipticity from the averaged well logs; 2) least-square fitting of non-hyperbolic synthetic travel-time curves parametrized by the following equation ([Alkhalifah and Tsvankin, 1995](#)):

$$t = \sqrt{t_0^2 + \frac{x^2}{V_{nmo}^2} - \frac{2\eta x^4}{V_{nmo}^2(t_0^2 V_{nmo}^2 + (1 + 2\eta)x^2)}}, \quad (4)$$

where  $t_0$  – travel-time at zero-offset,  $x$  – offset,  $V_{nmo}$  – moveout velocity. The equation is valid for weak anisotropy approximation and is accurate for large-offset-to-depth ratios.

Figure 4 demonstrates the anisotropy estimates by both approaches on an example of the Withnell 1 model. The anellipticity  $\eta = 0.28$  facilitates the best fit of a non-hyperbolic travel-time curve at the depth level of 1000 m. (Figure 4a). Nearly the same value of  $\eta$  is predicted by Backus theory (Figure 4c).

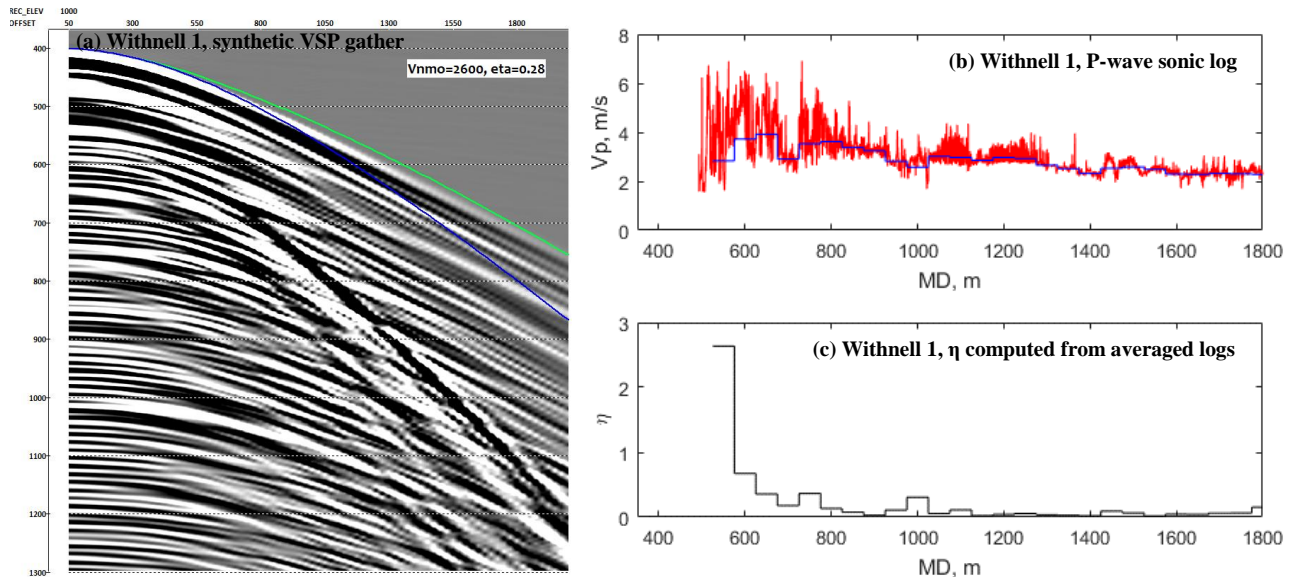


**Figure 4. Withnell 1 model.** (A) Synthetic common receiver VSP gather (receiver depth – 1000 m); vertical axis – time in ms; horizontal axis – source offset in m. Blue and green colours indicate hyperbolic and best-fit non-hyperbolic travel-time curves accordingly for  $V_{nmo} = 2600$  m/s. (B) Initial (red) and averaged (blue) P-wave sonic log. (C) Anellipticity  $\eta$  block-model computed from the averaged sonic and density logs.

For the chosen log averaging windows from 25 m to 40 m, anisotropy estimates obtained by Backus theory and least-square fitting are in a good agreement with each other. Parker 1 exhibits VTI anisotropy in the interval 625–1200 m with the average  $\eta$  around 0.3 peaking to  $\eta \approx 1.5$  at 850–875 m. Dampier 1 is characterized by the average  $\eta$  around 0.2 at 325–1000 m with the maximum  $\eta \approx 1$  at 540–565 m and 590–615 m. Bedding of Wilcox 2 borehole is less anisotropic compared to the other wells with the average  $\eta \approx 0.1$  at 850–1400 m and the maximum  $\eta \approx 0.25$  at 875–890 m.

## VSP CORRIDOR STACK

One of the objectives of the synthetic study was to examine how the bedding-induced attenuation affects a stacked reflection image. For that purpose, we compared the VSP corridor stack versus the trace obtained by a simple convolution of the reflectivity function with the pulse signature (Figure 5). The latter synthetics do not incorporate energy losses on wavefront divergence, transmission and frequency-dependent 1D scattering (bedding-induced attenuation) and thus can be used as reference data.

The vertical component of the near-zero-offset VSP seismogram (source offset of 50 m) was utilized for stacking. The data were scaled by a divergence factor, then the downgoing wavefield was suppressed in the FK-domain and the upgoing reflections were stacked using the NMO velocity function. To omit stacking with noise (surface multiples, converted waves), the traces were summed up over a window (corridor) in the vicinity of the first break times.

The presented time interval (Figure 5) corresponds to the depths below the section of high-contrast carbonate layers. From the figure we see that the VSP stack has drastically lower resolution and weaker intensity of the reflectors. We explain the observed effects by 1D scattering and transmission losses of seismic waves at the overlayering stiff carbonates.

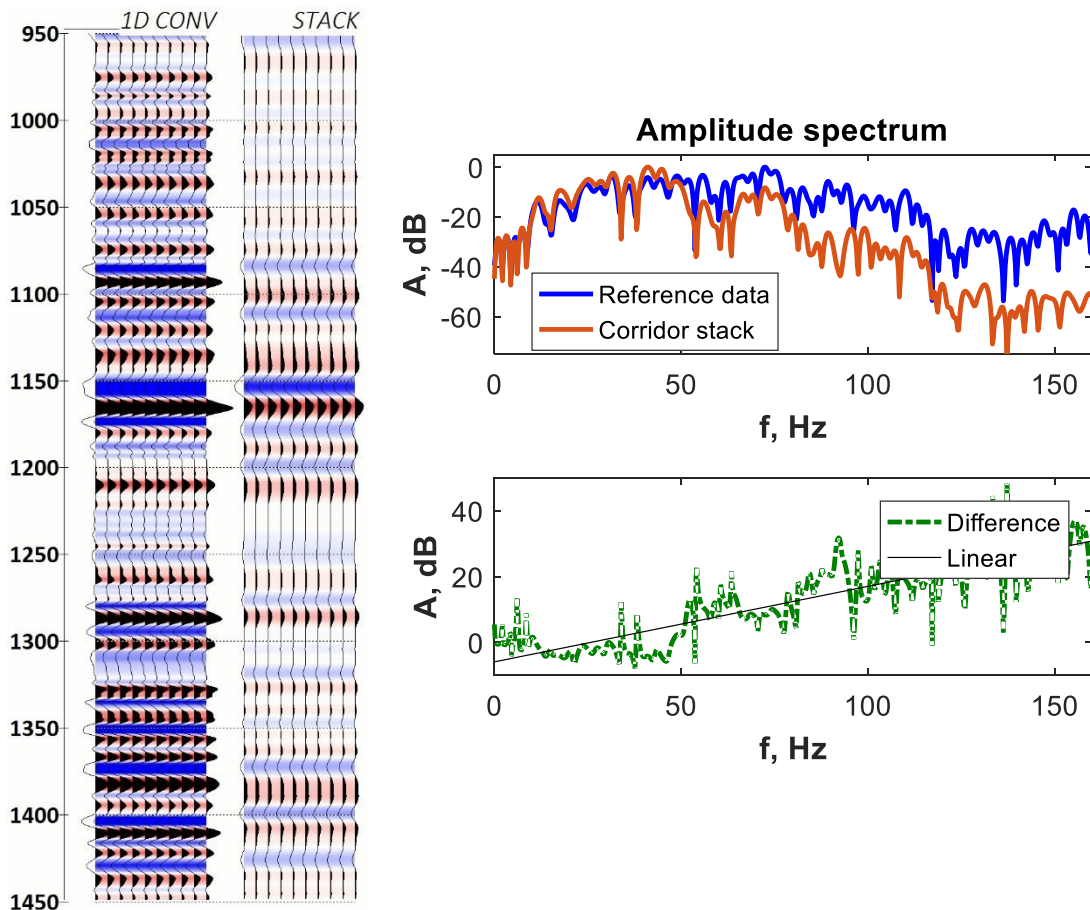


**Figure 5. Comparison of the reference data versus the VSP corridor stack constructed from the full-wave synthetics. Vertical axis on the left is in ms.**

## CONCLUSIONS

Full-wave seismic modelling for the flat-layered elastic models constructed from the logs of four wells revealed that the stiff finely-layered carbonates, which build up the overburden of the Northern Carnarvon basin, induce prominent scattering of seismic waves (frequency-dependent apparent attenuation) and VTI-anisotropy.

The attenuation in the Parker 1, Dampier 1, Wilcox 2 boreholes is described by a Q-factor from 75 to 100, which corresponds to the maximum drop of a centroid frequency around 6 Hz (for one-way propagation). Withnell 1 stands out from the other wells with drastically larger attenuation of  $Q \approx 7$ . This can be explained by very high contrast between the adjacent layers ( $> 100\%$ ) in the Withnell 1 model, whose density profile was built from the sonic logs using the Gardner equation.

It was shown that scattering attenuation caused by the carbonates in the overburden significantly affects resolution and intensity of the VSP corridor stack, which is a good proxy of a seismic stack.

The bedding-induced VTI-anisotropy described by anellipticity  $\eta$  varies from 0.1 to 1.5 in the intervals associated with high-contrast carbonate formations. This leads to a substantial non-hyperbolic moveout of reflected waves and should be taken into account in case full-offset seismic imaging is envisaged.

Finally, this paper provides a useful workflow for the synthetic study of 1D (layer-induced) effects on seismic wave propagation for 2D walk-away VSP and surface seismic survey geometries.

#### ACKNOWLEDGMENTS

We thank the sponsors of the Curtin Reservoir Geophysics Consortium (CRGC) for their financial support.

#### REFERENCES

- Alkhalifah, T., and Tsvankin, I., 1995, Velocity analysis for transversely isotropic media: *Geophysics*, 60, 1550-1566.
- Backus, G. E., 1962, Long-Wave Elastic Anisotropy Produced by Horizontal Layering: *J. Geophys. Res.*, 67, 4427-4440.
- O'Doherty, R. F., and Anstey, N. A., 1971, Reflections On Amplitudes: *Geophysical Prospecting*, 19, 430-458.
- Pevzner, R., Muller, T., Galvin, R., and Gurevich, B., 2012, Estimation of attenuation from zero-offset VSP data: CO2CRC Otway Project case study: *SEG Technical Program Expanded Abstracts*, 31
- Quan, Y. L., and Harris, J. M., 1997, Seismic attenuation tomography using the frequency shift method: *Geophysics*, 62, 895-905.
- Schmidt, H., and Tango, G., 1986, Efficient global matrix approach to the computation of synthetic seismograms: *Geophysical Journal of the Royal Astronomical Society*, 84, 331-359.
- Tsvankin, I., 2012, Seismic Signatures and Analysis of Reflection Data in Anisotropic Media, Third Edition: *Geophysical References Series*, Society of Exploration Geophysicists